Computing the electric field from Extensive Air Showers using a realistic description of the atmosphere

Benoît Revenu, F. Gaté, V. Marin, Richard Dallier, A. Escudie, D. García-Fernández, Lilian Martin

PROCEEDINGS OF SCIENCE

Computing the electric field from Extensive Air Showers using a realistic description of the atmosphere

B. Revenu[1,3], **F. Gaté**[1], **V. Marin**[2], **R. Dallier**[1,3], **A. Escudie**[1], **D.García-Fernández**[1], **L. Martin**[1,3]

[1] *Subatech, Institut Mines-Telecom Atlantique, CNRS, Universite de Nantes, Nantes, France*
[2] *Nantes, France*
[3] *Unité Scientifique de Nançay, Observatoire de Paris, CNRS, PSL, UO/OSUC, Nançay, France*
E-mail: revenu@in2p3.fr

The composition of ultra-high energy cosmic rays is still poorly known and this is an very important topic in the field of high-energy astrophysics. We detect them through the extensive air showers they create after interacting with the atmosphere constituents. The secondary electrons and positrons of the showers emit an electric field in the kHz-GHz range. It is possible to use this radio signal in 20-80 MHz for the estimation of the atmospheric depth of maximal development of the showers $X_{\max}$, with a good accuracy and a duty cycle close to 100%. This value of $X_{\max}$ is strongly correlated to the nature of the primary cosmic ray that initiated the shower. We present the importance of using a realistic atmospheric model in order to correct for systematic errors that can prevent a correct and unbiased estimation of $X_{\max}$.

35th International Cosmic Ray Conference — ICRC2017
10–20 July, 2017
Bexco, Busan, Korea

PoS(ICRC2017)573

1. Introduction

In the last years, most of the air shower detection experiments run arrays of radio detectors in order to measure the electric field emitted by showers. Antennas are commonly used in the band 30-80 MHz where the electric field is coherently emitted by all secondary electrons and positrons. Detecting this field is now routinely achieved but more difficult is extracting the primary cosmic ray characteristics using this radio signal. This is done with simulations codes such as [1, 2, 3]. They compute the expected electric field as a function of time and of the observer's location with respect to the shower axis. They rely on the choice of the nature of the primary cosmic ray (light or heavy nucleus), its energy and the shower geometry (zenith and azimuthal angles). Then, secondary particles are created and tracked; they evolve in the atmosphere, generally described by its density $\rho_{\rm air}$, as a function of the altitude z. The atmospheric depth $X = \int \rho_{\rm air}(z)\mathrm{d}z$ is a critical quantity as it describes the shower development in the air and represents the amount of matter crossed by the particles. Taking the example of the code SELFAS, we compute the atmospheric depth by numerical integration, taking into account the curved shape of the Earth and its atmosphere; we don't use anymore the flat approximation which is valid up to 60°. The (new) SELFAS electric field formula is (see [4]):

$$\mathbf{E}(\mathbf{x},t) = \frac{1}{4\pi\varepsilon}\int \mathrm{d}^3x' \left\{ \left[\frac{\rho(\mathbf{x}',t_{\rm ret})\mathbf{r}}{R^2(1-n\beta\cdot\mathbf{r})}\right]_{\rm ret} + \frac{n}{c}\frac{\partial}{\partial t}\left[\frac{\rho(\mathbf{x}',t_{\rm ret})\mathbf{r}}{R(1-n\beta\cdot\mathbf{r})}\right]_{\rm ret} - \frac{n^2}{c^2}\frac{\partial}{\partial t}\left[\frac{\mathbf{J}(\mathbf{x}',t_{\rm ret})}{R(1-n\beta\cdot\mathbf{r})}\right]_{\rm ret}\right\}. \tag{1.1}$$

This is the electric field expression at the observer's location $\mathbf{x}$ at time t from the charge density ρ, current $\mathbf{J}$, $\mathbf{r}$ being the normalized vector particle-observer and $\mathbf{v} = c\beta$. R is the distance particle-observer. Integration is performed for retarded time $t_{\rm ret} = t - nR/c$. The air index n also plays an important role as it drives the electric field amplitude (in particular close to the Cherenkov angle) and the arrival time of the signal at the observer's location, i.e. the pulse shape. For those reasons, it is very important to describe the atmosphere accurately enough.

2. Atmospheric model

The atmosphere is a layer of gas around the Earth. The properties of this gas are more or less stable according to the time of the day (daily effect) and the time of the year (seasonal effect). A rough description assumes the atmosphere is in a steady state at fixed altitude; this is the case for the US Standard model [5]. A much more detailed, and updated model is provided by the Global Data Assimilation System (GDAS) [6].

2.1 The US Standard atmosphere

This model exists since 1976 and is an idealized representation of the atmosphere from the sea level up to 1000 km of altitude, in period of moderate solar activity. Values are estimated from yearly averages under the assumption of hydrostatic equilibrium; air is considered as an homogeneous mixture of several gases. The US Standard air density profile can be retrieved easily from [7] as large table; analytic formulas are also available, using 4 ou 5 atmospheric layers with continuity conditions, as it is the case for the Linsley parameterization. The US Standard atmosphere provides for instance, $\rho_{\rm air}(z)$ as an average value for all locations on the Earth, be it in winter or summer, day

or night. We can expect quite large deviations with respect to specific weather conditions that can be very different from the US Standard values: it should also have an impact on the electric field emitted by showers during those specific weather conditions. The SELFAS code used the Linsley parameterization up to December, 2016. It can also use a much more refined model, based on the GDAS.

2.2 The GDAS model

The GDAS is the system used by US official agencies (such as the National Center for Environmental Prediction, the Global Forecast System) "to place observations into a gridded model space for the purpose of starting, or initializing, weather forecasts with observed data" (see [8]). The resulting 3D model space uses various ground observations, balloon data, wind profiler data, aircraft reports, buoy, radar and satellite data. This model can be retrieved on grid of various size in terms on longitude and latitude ($1^\circ \times 1^\circ$, $0.5^\circ \times 0.5^\circ$ or even $0.25^\circ \times 0.25^\circ$) starting from year 2001. The timestep for these data is 3 hours. It is possible to get the 3D model for the actual atmospheric conditions for any location on Earth at any time, up to an altitude of $z_{\rm max}^{\rm GDAS} = 26$ km. Many variables are available in the GDAS model. Four our needs, we will focus on the variables driving the values of interest ($\rho_{\rm air}$ and n) for the electric field computation: the relative humidity (R_h), the temperature (T) and the total pressure (P). Using such a refined model is a good approach as the data show large deviations, see for instance in FIG. 1 the relative humidity as a function of the altitude for the location of Nançay, France on March 18, 2014. At fixed altitude, the variations

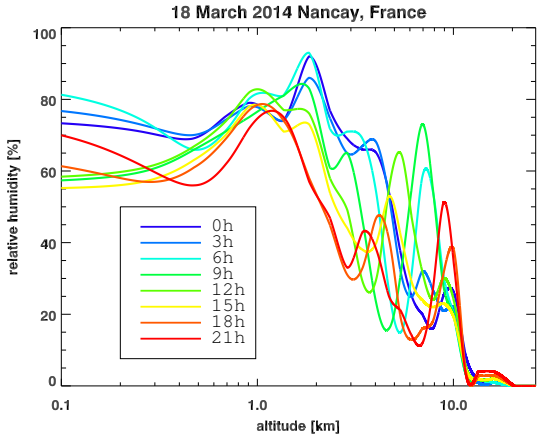

Figure 1: Daily variations of the relative humidity as a function of the altitude, using the GDAS data at Nançay on March 18, 2014.

during the day are very important; the relative humidity has a role in the value of the air refractive index so that we also expect an influence on the electric field from air showers compared to a "standard" and constant relative humidity.

The idea is to compute the atmosphere density $\rho_{\rm air}$ and air index n at the time and location an event is detected. Then, the shower can be simulated with SELFAS, running with the corresponding atmosphere at the time of detection. The simulation will be done with the best astmospheric model possible, on a case-by-case basis. In order to compute accurately $\rho_{\rm air}$ and n, the procedure consists

in using the pressure (in hPa), the temperature (in K) and the relative humidity (in %) as a function of the geopotential height G_h in geopotential meters (gpm). We convert these meters into altitude above sea level. Then, the air density ρ_{air} is computed from the ideal gas law:

$$\rho_{\text{air}}(z) = \frac{p_d(z(Z_g,\phi))M_d + p_v(z(Z_g,\phi))M_v}{RT(z(Z_g,\phi))}, \tag{2.1}$$

where $z(Z_g,\phi)$ is the altitude above sea level corresponding to the geopotential height Z_g at a latitude ϕ; p_d and p_v are the partial pressures of dry air and water vapor and M_d and M_v the molar masses. The water vapor partial pressure is given by $p_v = R_h p_{\text{sat}}$ where p_{sat} is given by (see [9, 10]):

$$p_{\text{sat}} = 6.1121 \exp\left[\left(18.678 - \frac{T}{234.5}\right)\left(\frac{T}{257.14+T}\right)\right] \quad (T \text{ in } ^\circ\text{C}). \tag{2.2}$$

Then, $p_d = P - p_v$. This equation can be used in the range $[-80;+50]^\circ$C, which is our range of interest.

We have the recipe to compute all relevant quantities to simulate accurately the electric field emitted by air showers using the GDAS data, provided only up to $z_{\text{max}}^{\text{GDAS}} = 26$ km above sea level. As air showers can initiate at much larger altitudes, we use the US Standard model with a scaling factor to ensure continuity with the GDAS model below $z_{\text{max}}^{\text{GDAS}}$, up to an altitude of ~ 110 km, which is considered as the limit of the atmosphere.

Finally, we get an accurate atmosphere model for the time of the detection of an event, at any place in the world, using both the GDAS data below $z_{\text{max}}^{\text{GDAS}}$ and the rescaled US Standard model between $z_{\text{max}}^{\text{GDAS}}$ and 110 km. FIG. 2 presents the maximum relative differences $(\rho_{\text{GDAS}} - \rho_{\text{US}})/\rho_{\text{US}}$ as a function of the altitude, between the GDAS model and the US Standard model during the year 2014 in Nançay. We also show the relative difference for the sample day March 18, 2014. We see

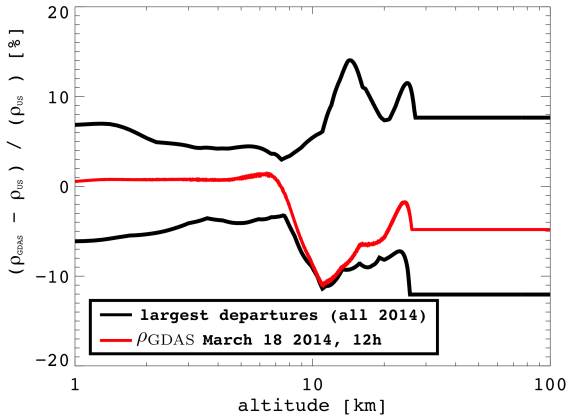

Figure 2: In black: extrema of the differences between the US Standard model air density profile and all the GDAS profiles along the year 2014, as a function of altitude. In red: the air density computed from the GDAS model on March 18, 2014.

that the relative differences can reach $\pm 15\%$, which will have a large influence of the atmospherical depths.

3. Effect on the electric field computation

In order to check directly the influence of the chosen atmospheric model, we simulated a shower with SELFAS, initiated by a 1 EeV proton with a first interaction depth $X_1 = 100$ g/cm^2, a zenith angle $\theta = 30^\circ$ and azimuth $\phi = 90^\circ$ (coming from the North). We compute the total electric field amplitude as a function of the axis distance and in the direction of $\mathbf{v} \times \mathbf{B}$, where $\mathbf{v}$ is the shower axis direction and $\mathbf{B}$ the geomagnetic field at the observer's location. We did this simulation considering the US Standard atmosphere and taking the actual atmosphere on March 18, 2014, in Nançay. The electric field amplitudes are shown in FIG. 3. We observe that the electric field profile

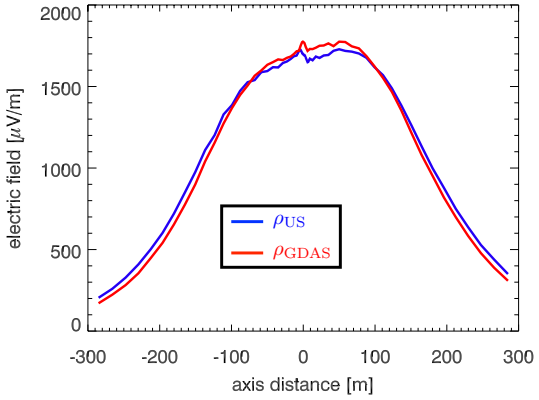

Figure 3: Total electric field amplitude in the shower front reference frame as a function of the axis distance in the direction $\mathbf{V} \times \mathbf{B}$, where $\mathbf{V}$ is the shower axis and $\mathbf{B}$ the geomagnetic field. This corresponds to a the same shower initiated by a proton at 1 EeV with a first interaction depth of 100 g/cm^2, $\theta = 30^\circ$ and $\phi = 90^\circ$, developing once in US Standard model (blue curve) and once in the atmospheric model based on the GDAS data on March 18, 2014 at noon (red curve).

is larger when considering the US Standard model which is a source of systematic error when trying to reconstruct the $X_{\max}$ from the radio signal. We can imagine a reversed situation where the simulated profile is larger in the GDAS case. This emphasize the importance of considering the actual atmosphere at the time of detection of an event.

4. Air index computation

The other fundamental parameter to properly estimate for the electric field computation is the air index. Let's consider a secondary charged particle of the shower at an altitude z and a distance R from the observer. The electric field amplitude depends directly on n as explicited in EQ. 1.1. Then, the arrival time t of the wave at the observer's location is $t = t_e + < n > R/c$ where t_e is the emission time and $< n >$ is the average value of the air index on the line particle-observer. Usually, the air index is provided by the Gladstone and Dale law:

$$n(z(l)) = 1 + \kappa \rho(z(\ell)) \text{ with } \kappa = 0.226 \text{ cm}^3/\text{g}. \tag{4.1}$$

The corresponding average air index $< n >$ is given by:

$$< n(z(\ell)) >= 1 + \frac{\kappa}{\ell} \int_0^\ell \rho(z(\ell'))\, \mathrm{d}\ell'$$

But the Gladstone and Dale constant κ depends on the medium and on the considered wavelength. We used in SELFAS (up to December 2016) the same value than that in use in CoREAS: the constant $\kappa = 0.226$ cm^3/g corresponds to optical wavelengths ($\lambda \sim 400$ nm). This is not suited for our MHz frequency range: $\lambda = 7.5$ m at 40 MHz. A more suited approach is to properly take into account the humidity fraction R_h which plays an important role in the value of the air index according to [11]:

$$n = 1 + 10^{-6} N \quad \text{with} \quad N = \frac{77.6}{T}\left(P + 4810\,\frac{p_v}{T}\right) \qquad T \text{ in K}, \tag{4.2}$$

where N is the refractivity. This equation is proposed for the MHz to GHz domain. The air density is hidden in T and P as we assume the ideal gas law approximation is valid. It means that the refractivity will be different when considering a GDAS model or the US Standard model. The water vapor partial pressure explicitly appears and can be the dominant term: the air refractive index should be computed with this parameter. As in section 2.2, we can use the accurate formula using the GDAS data up to $z_{\max}^{\mathrm{GDAS}}$. Beyond this altitude, we have no data for temperature and relative humidity. Hopefully, the air relative humidity beyond $z_{\max}^{\mathrm{GDAS}}$ can be considered as null as usually no clouds are observed above 12 km. We can therefore use a simpler formula above $z_{\max}^{\mathrm{GDAS}}$:

$$p_v = 0,\ P = p_d,\ T = \frac{P_d M_d}{R\rho} \quad \text{so that} \quad N = 77.6\,\frac{R\rho}{M_d} \quad \text{with} \quad \rho = \rho_{\mathrm{US}},$$

the ρ_{US} being the rescaled US Standard density ensuring continuity with ρ_{GDAS} at $z_{\max}^{\mathrm{GDAS}}$. The difference between the air refractivity N in the US Standard atmosphere and in the GDAS model is shown in FIG. 4. We see that the relative difference can reach 35% close to the ground (where

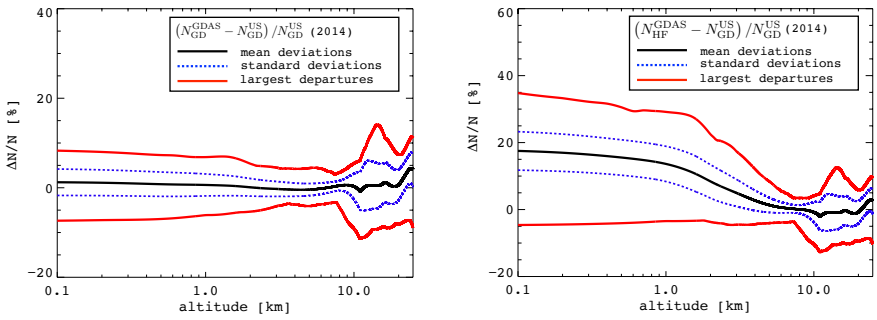

Figure 4: Relative difference in refractivity as a function of the altitude, with respect to the case $N_{\mathrm{GD}}^{\mathrm{US}}$, for $N_{\mathrm{GD}}^{\mathrm{GDAS}}$ (left) and $N_{\mathrm{HF}}^{\mathrm{GDAS}}$ (right). The black line corresponds to the mean values for the year 2014 and the red lines correspond to the maximum deviations. The largest deviations in the $N_{\mathrm{HF}}^{\mathrm{GDAS}}$ case (right) correspond to the high level of humidity below $5-6$ km of altitude. The blue dashed line indicates the standard deviation of the relative difference.

the humidity fraction can be very large) and around 15% at altitudes of interest for the shower

development (10-20 km). As the refractivity appears with a 10^{-6} factor in the air index, the effect on the electric field is not so important, as shown in FIG. 5. In this figure, we show the electric field in the three polarizations East-West, North-South and vertical as a function of time for a shower initiated by a 1 EeV proton with $X_1 = 100$ g/cm^2 and $\theta = 30°$, $\phi = 90°$, for observers located at different positions around the shower axis. The only difference is the value of the refractivity: we consider the value using the US Standard atmosphere with the Gladstone and Dale law in one case and the GDAS model on March 18, 2014 with the high frequency formula (EQ. 4.2) in the other case. We see that the North-South amplitude can be modified by 30% and the arrival time of the

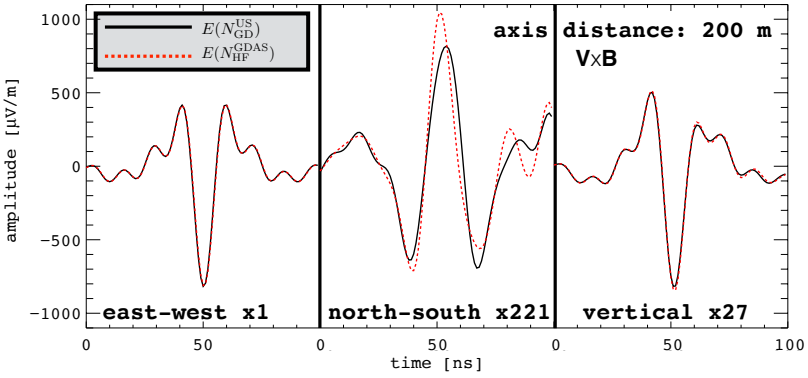

Figure 5: Time series of the electric field simulated with SELFAS using N_{HF}^{GDAS} in red and N_{GD}^{US} in black, with the same air density profile, at 200 m from the shower axis in the polarization parallel to $\mathbf{v} \times \mathbf{B}$. The shower is induced by a proton at 1 EeV with a first interaction depth of 100 g/cm^2, $\theta = 30°$, $\phi = 90°$; the electric field is filtered in the band $[20;80]$ MHz using the three polarizations that are indicated at the bottom of each plot together with the scale factor applied for better visibility.

wave at the observer location can be shifted by 5 ns. In this example, the East-West amplitude is dominant so that the total electric field will not be strongly affected by the choice of the air index model. But if the considered experiment does not measure all three polarizations then the choice of the model is primordial.

5. Unbiased X_{max} reconstruction

In this section we check the estimation of the X_{max} in the context of the choice of the atmospheric model. For this, we simulate a shower on March 18, 2014 initiated by a 1 EeV proton with $X_{max} = 720$ g/cm^2 and $\theta = 30°$, $\phi = 90°$. This is our reference event, the one we want to reconstruct. We then apply the same procedure as we do with actual cosmic events. We simulate showers initiated by protons and iron nuclei having the same arrival direction and energy but random X_{max}. One set of protons and iron nuclei showers uses the US Standard air density and the corresponding refractivity N_{GD}^{US}. The other set uses the same atmosphere than our reference event (on March 18, 2014) with the refractivity N_{HF}^{GDAS}. As described in [12], the agreement between each simulated electric field and the mock data of the test event is tested with a χ^2 test. The preferred X_{max} value is 750 g/cm^2 when using the US Standard atmosphere. It is 718 g/cm^2 when using the GDAS atmosphere at the time of detection of the event. The true value is 720 g/cm^2. The

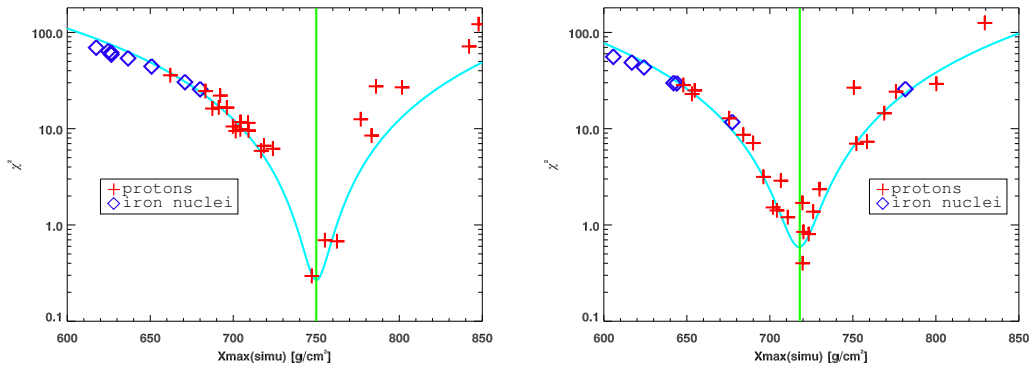

Figure 6: Value of the χ^2 test as a function of the simulated $X_{\max}$ depths for the set of showers simulated using ρ_{US} and $N_{\text{GD}}^{\text{US}}$ (top) and the set of showers using ρ_{GDAS} and $N_{\text{HF}}^{\text{GDAS}}$ (bottom).

discrepancy between the two models is due to the choice of the atmospherical model. It is very important to note that when converting atmospherical depths to distances to the point of maximum emission, both models leads to the same value of 4380 m from the shower core. It means that the electric field distribution is governed by the geometrical distance to the observer and not directly by the atmospherical depth. It also means that the preferred electric field distribution in the two data sets corresponds to showers having their maximum emission at the same distance to the observer and not at the same $X_{\max}$. In other words, using different atmospheric models allow to reconstruct directly, with no bias, the correct $X_{\max}$. This is not possible using the US Standard model which gives in this example a value shifted by 30 g/cm^2 with respect to the true value.

6. Conclusion

We have studied the importance of using a precise model of the atmosphere in the context of the computation of the electric field emitted by air showers during their development. The air density ρ_{air} and air index n are influenced by the weather conditions. Two models are available: the US Standard description which provides average atmosphere characteristics; these are the same for all locations on the Earth and any time (day/night, winter/summer). The other one is based on the GDAS model which allows an accurate atmosphere estimation at the time an event is detected. We have shown that the relative difference in the air density can reach $\pm 15\%$ between both models. This can lead to differences up to some tens of g/cm^2 in terms of atmospheric depths. This is clearly not negligible as the uncertainty on the $X_{\max}$ using the radio technique is of the order of 20 g/cm^2. The air index value is also driven by the atmospheric model: its density but also the humidity fraction which can have a dominant influence on the refractivity. The Gladstone and Dale law is commonly used but it is not suitable for our frequency range and does not take into account the humidity fraction. Considering a basic refractivity model (with the US Standard atmosphere and the Gladstone and Dale law) and an accurate refractivity model (properly using both the GDAS model and the humidity fraction), we have shown that the electric field is altered by the model: amplitudes can be modified by some tens of % and the arrival time of the wave at the observer

location can be shifted by some ns. This should be of relative importance according to the specific design of the considered experiment. Finally, we compared the $X_{\max}$ estimation using a reference event simulated using the atmosphere of a specific day, with a true value of $X_{\max} = 720$ g/cm^2. We used two simulated sets of showers initiated by protons and iron nuclei of the same energy and arrival direction than the reference event but with random $X_{\max}$. One set uses the US Standard atmosphere and the Gladstone and Dale law; the other one uses the same atmosphere than that of the reference event, together with the refined air index model. The first set leads to a biased $X_{\max}$ estimation of 750 g/cm^2 and the second one to a correct value of 718 g/cm^2. Using a crude atmosphere model leads to biased $X_{\max}$ values, up to some tens of g/cm^2. Nevertheless, their is no bias on the distance to the shower maximum emission point: US Standard and $X_{\max} = 750$ g/cm^2 correspond to the same distance than GDAS and $X_{\max} = 718$ g/cm^2. The conversion can be done afterwards but it is clearly better to run the shower simulation directly in the best atmospheric model in order to properly consider all effects into account (correct atmospheric depths and correct air index).

References

[1] Vincent Marin *et al. Simulation of radio emission from cosmic ray air shower with SELFAS2*. *Astropart.Phys.*, 35:733–741, 2012.

[2] J. Alvarez Muñiz *et al. Monte Carlo simulations of radio pulses in atmospheric showers using ZHAireS*. *Astropart. Phys.*, 35:325–341, 2012.

[3] T. Huege *et al. Full Monte Carlo simulations of radio emission from extensive air showers with CoREAS*. In *proceedings of the 33rd ICRC, Rio de Janeiro, Brasil*, number id 548. arXiv:1307.7566, July 2013.

[4] D. García-Fernández et al. *Near-field radio emission induced by extensive air showers*. In *this conference*.

[5] NASA NOAA. *https://ntrs.nasa.gov/archive/nasa/casi.ntrs.nasa.gov/19770009539.pdf*. Technical report, 1976.

[6] *GDAS Archive Information, http://ready.arl.noaa.gov/gdas1.php*. Technical report, NOAA.

[7] *http://www.digitaldutch.com/atmoscalc/table.htm*. Technical report.

[8] NASA NOAA. *https://www.ncdc.noaa.gov/data-access/model-data/model-datasets/global-data-assimilation-system-gdas*. Technical
report.

[9] A. L. Buck. *New equations for computing vapor pressure and enhancement factor*. *J. Appl. Meteorol.*, (20):1527:1532, 1981.

[10] A. L. Buck. *Buck Research CR-1A User's Manual*. Technical report, 1996.

[11] R. L. Freeman. *Radio System Design for Telecommunications, Third Edition*. 2006.

[12] F. Gaté *et al.* X_{max} *reconstruction from amplitude information with AERA*. In *Proceedings of the ARENA 2016 workshop (Groningen, The Netherlands)*. ARENA, 2016.